Bull. Korean Math. Soc. **54** (2017), No. 6, pp. 1893–1912
https://doi.org/10.4134/BKMS.b160240
pISSN: 1015-8634 / eISSN: 2234-3016

A NONSTANDARD FINITE DIFFERENCE METHOD APPLIED TO A MATHEMATICAL CHOLERA MODEL

Shu Liao and Weiming Yang

Abstract. In this paper, we aim to construct a nonstandard finite difference (NSFD) scheme to solve numerically a mathematical model for cholera epidemic dynamics. We first show that if the basic reproduction number is less than unity, the disease-free equilibrium (DFE) is locally asymptotically stable. Moreover, we mainly establish the global stability analysis of the DFE and endemic equilibrium by using suitable Lyapunov functionals regardless of the time step size. Finally, numerical simulations with different time step sizes and initial conditions are carried out and comparisons are made with other well-known methods to illustrate the main theoretical results.

1. Introduction

cholera is an acute intestinal infection, caused by ingestion of food or water which is contaminated with a number of types of Vibrio cholerae, remains a significant threat to public health for most of the developing countries with poor sanitation, crowding, war, and famine in the past few years, such as in Congo (2008), in Iraq (2008), in Zimbabwe (2008-2009), in Vietnam (2009), in Kenya (2010), in Nigeria (2010), in Haiti (2010), in Mexico (2013), and most recently in South Sudan (2014). According to the World Health Organization (WHO) [40] report (2010), cholera has become an acute disease throughout the world since 1961 and causes 58,000-130,000 deaths a year. In the last few decades, enormous attention has been paid to the cholera disease and a number of mathematical models have been contributed to a better understanding of the transmission of cholera. In 2001, Codeço [10] put an emphasis on the decisive importance of the environmental component and proposed a $SIRB$

Received March 21, 2016; Revised June 9, 2017; Accepted June 26, 2017.
2010 *Mathematics Subject Classification.* Primary 34D20, 92D30.
Key words and phrases. cholera, nonstandard finite difference scheme, dynamical systems, global stability.
This work was partially supported by the Natural Science Foundation of China (11401059), the Natural Science Foundation of CQ (cstc2015jcyjA00024, cstc2017jcyjAX0067), Scientific and Technological Research Program of Chongqing Municipal Education Commission (KJ1600610, KJ1706163).

epidemic model in which B represents the *V. cholerae* concentration in water. Meanwhile, Hartley Morris and Smith [14] discovered a representative hyperinfectious state of the pathogen-the 'explosive' infectivity of freshly shed *V. cholerae* based on the laboratory results. In 2010, Tien and Earn [36] proposed a water-borne disease model with multiple transmission pathways: direct human-to-human and indirect water-to-human transmissions, identified how these transmission routes influence disease dynamics. Mukandavire *et al.* [29] in 2011 simplified Hartley's model to understand transmission dynamics of cholera outbreak in Zimbabwe. Liao and Wang [19] conducted a dynamical analysis of the Hartley's model to study the stability of both the disease-free and endemic equilibria so as to explore the complex epidemic and endemic dynamics of the disease. More papers in the field of cholera epidemic models are presented in ([8, 20, 27, 38]).

Nowadays, continuous-time cholera models have been widely studied by many scholars. However, it is necessary to discretize the continuous models for practical purposes. First of all, Villanueva *et al.* [37] in 2008 pointed out that numerical methods like traditional Euler, Runge-Kutta and some standard procedures of MATLAB software fail to solve nonlinear systems generating oscillations, chaos, and unsteady states if the time step size increases to a critical size. The second reason is that the results of the discrete time models are more accurate and convenient to describe infectious diseases and could preserve as much as possible the qualitative properties of the corresponding continuous models. Some useful studies can be found in the works of ([1–3, 9, 17, 33]). Sekiguchi and Ishiwata [34] obtained a discretized $SIRS$ epidemic model with time delay and the sufficient conditions for global behaviors of the solutions. The dynamical behaviors of a class of discrete-time $SIRS$ epidemic models were considered by Hu *et al.* [16] in 2012, their paper revealed that when the time step h is sufficiently small, the dynamical behaviors of discrete model are similar to the continuous-time model, whereas when h becomes large, the discrete model appears more complex dynamical behaviors, such as flip bifurcation, Hopf-bifurcation and chaos phenomenon. Muroya *et al.* [30] proposed a discrete epidemic model with immunity and latency spreading in a heterogeneous host population by using the backward Euler method, they also focused on proving the global asymptotic stability with the help of the Lyapunov function technique when $R_0 > 1$. Wang *et al.* [39] in 2013 studied a discrete $SIRS$ model with standard incidence rate, the sufficient conditions were obtained for the global attractivity of the endemic equilibrium by using the iteration technique and the comparison principle of difference equations. Ma *et al.* [21] studied a discrete SIR epidemic model and obtained some sufficient conditions for the global stability of the endemic equilibrium. At last, they applied the discrete model to study the mumps infection in China.

Although there are different approaches to model infectious diseases in discrete time, the nonstandard finite difference (NSFD) scheme developed by Mickens ([22–24]) is well known and has been applied to many articles in recent

years. In general, the NSFD method is rooted in an elementary set of directly and carefully designed laws aimed at preserving the most properties of the corresponding continuous-time system, such as positivity, boundedness, stability of equilibrium points, conservation law and others. An NSFD discretization must satisfy one of the following two conditions ([4, 5, 25, 26]): (1) nonlocal approximation is used. (2) discretization of derivative is not traditional and a denominator function $\phi(h) = h + o(h^2)$ is used. However, in some cases, more complex functions of the time step size are used to replace the classical one. Mickens [26] introduced that the use of NSFD scheme is always qualitatively the same asymptotic dynamics of continuous-time model. Villanueva *et al.* [37] developed an NSFD scheme to solve numerically a mathematical model for obesity population dynamics with constant population size. The numerical results in this paper showed the effectiveness of the proposed nonstandard numerical scheme by comparing with Euler's method and the fourth-order Runge-Kutta method. Jodar *et al.* [18] constructed an NSFD scheme for influenza, they showed the solutions of the discretized model have the same properties as the original continuous model. However, they didn't give the proof of the global stability. Arenas *et al.* [6] constructed and developed a competitive NSFD scheme of predictor-corrector type for the classical SIR epidemic model. Garba *et al.* [11] formulated two finite-difference methods, one is standard and the other is based on the non-standard discretization framework to solve the continuous-time model. The latter one can capture many essential qualitative features of the continuous-time model such as positivity and invariance of a solution, backward bifurcation, convergence to the correct equilibrium solution. Suryanto *et al.* [35] constructed an NSFD scheme to solve a SIR epidemic model with modified saturated incidence rate. From their numerical simulations, the NSFD scheme allowed large time step size to save the computational cost. Guerrero *et al.* [12] developed an NSFD scheme to solve the prevalence of smoking in Spain. They compared the NSFD scheme with Euler, trapezoidal and fourth-order Runge-Kutta methods to conclude that the NSFD was a good option to solve the mathematical model numerically .

In this paper, motivated by the above studies, we will apply NSFD discretization method to solve the prevalence of cholera outbreak in Zimbabwe (2008-2009), the continuous-time cholera model is originally presented in Mukandavire *et al.* [29]. It must be pointed out that the model in [29] is purely under the idealized condition that the population always remains a constant and the natural birth and death rates are assumed equal, which may not be true in the real world. However, when the disease mortality is included and different natural birth and death rates are applied, the total population will vary in time. Thus, we will make two modifications of the original model in Mukandavire *et al.* [29], one of which is to enter the susceptible population at any moment is rate Λ, and the other of which is to define the rate of disease-related death.

To our knowledge, this is the first time to design dynamically consistent nonstandard finite difference scheme to study cholera model. In addition, we

notice that much research has only been done on the global stability of the continuous cholera models, the results on the global stability of the equilibria for discrete models are quite few because discrete models always exhibit much more complicated dynamical behaviors, we will solve this difficulty by using suitable Lyapunov functions in the present paper.

The paper is organized as follows. In Section 2, we modify the continuous model for describing cholera epidemic which is originally developed by Mukandavire *et al.* [29], where some of its basic dynamical features are presented. In Section 3, we construct a discretized cholera model from the continuous model by using the nonstandard finite difference method. The stability properties of the disease-free and the endemic equilibria are discussed in Section 4 and Section 5. In Section 6, numerical simulations are carried out to test the numerical stability of this NSFD scheme and performance versus other well-known schemes. Finally, we close the paper by a discussion in Section 7.

2. ODE model

In this section, we modify the mathematical model which is originally developed by Mukandavire *et al.* [29] to understand the transmission dynamics and ecology of cholera in Zimbabwe (2008-2009). The transmission of cholera epidemic is different from other diseases since it involves multiple transmission pathways: both direct human-to-human and indirect environment-to-human transmissions, thus susceptible population infect cholera either from contaminated water at rate $\frac{\beta_e B}{\kappa+B}$ or from the ingestion of hyperinfectious vibrios at rate $\beta_h I$, respectively. We consider the following system of nonlinear ordinary differential equations:

$$\frac{dS}{dt} = \Lambda - \beta_e \frac{SB}{\kappa + B} - \beta_h SI - \mu S, \tag{1}$$

$$\frac{dI}{dt} = \beta_e \frac{SB}{\kappa + B} + \beta_h SI - (\gamma + \mu + u_1)I, \tag{2}$$

$$\frac{dB}{dt} = \xi I - \delta B, \tag{3}$$

$$\frac{dR}{dt} = \gamma I - \mu R, \tag{4}$$

where S, I and R denote the susceptible, the infected, and the recovered populations, respectively; B denotes the density of *V. cholerae*. We assume that new recruits including newborns, travel, etc. enter the susceptible population at any moment is a constant rate Λ ([13,15,41]). β_h and β_e denote the concentrations of the hyperinfectious (HI) and less-infectious (LI) vibrios, respectively. μ represents the natural death rate that is not related to the disease, u_1 defines the rate of disease-related death, κ is the concentration of vibrios in contaminated water in the environment, ξ the natural decay rate of *V. cholerae*, δ the bacterial death rate, and γ the recovery rate. All the parameters are strictly

positive constants. The initial conditions of the system (1)-(4) are assumed as following:

$$S \geq 0, I \geq 0, B \geq 0, R \geq 0. \tag{5}$$

According to Mukandavire's work, we summarize some dynamical properties of the continuous model (1)-(4). The basic reproductive number R_0 can be calculated easily as:

$$R_0 = \frac{\Lambda(\xi\beta_e + \delta\kappa\beta_h)}{\mu\delta\kappa(\gamma + \mu + u_1)}. \tag{6}$$

It can further be proved that disease-free equilibrium E_0 and endemic equilibrium E^* have the following stability properties:

Theorem 2.1. *The disease-free equilibrium of the model system* (1)-(4)*, given by* $E_0 = (\frac{\Lambda}{\mu}, 0, 0, 0)$*, is locally asymptotically stable and globally asymptotically stable whenever* $R_0 < 1$*.*

Theorem 2.2. *The endemic equilibrium of the model system* (1)-(4)*, given by* $E^* = (S^*, I^*, B^*, R^*)$*, where*

$$\begin{aligned} S^* &= \frac{\Lambda}{\mu} - \frac{(\gamma + \mu + u_1)I^*}{\mu}, \\ I^* &= \frac{\beta_e S^*}{\gamma + \mu + u_1 - \beta_h S^*} - \frac{\delta\kappa}{\xi}, \\ B^* &= \frac{\xi I^*}{\delta}, \\ R^* &= \frac{\gamma I^*}{\mu}, \end{aligned}$$

is locally asymptotically stable and globally asymptotically stable whenever $R_0 > 1$*.*

3. The NSFD scheme

In general, the discrete epidemic models obtained by Mickens-type discretization have the same features as the original continuous-time model ([31, 32]). In this section, we construct a dynamically consistent numerical NSFD discrete scheme for solving system (1)-(4).

Let us denote $t_n = nh$, with n integer, $h = t_{n+1} - t_n$ be the time step size, and let S_n, I_n, B_n, and R_n be the approximated values of the variables S_{nh}, I_{nh}, B_{nh} and R_{nh}, respectively. Thus, the NSFD scheme for the model system (1)-(4) takes the following form

$$\frac{S_{n+1} - S_n}{\phi(h)} = \Lambda - \beta_e \frac{S_{n+1}B_n}{\kappa + B_n} - \beta_h S_{n+1} I_n - \mu S_{n+1}, \tag{7}$$

$$\frac{I_{n+1} - I_n}{\phi(h)} = \beta_e \frac{S_{n+1}B_n}{\kappa + B_n} + \beta_h S_{n+1} I_n - (\gamma + \mu + u_1) I_{n+1}, \tag{8}$$

$$\frac{B_{n+1}-B_n}{\phi(h)} = \xi I_{n+1} - \delta B_{n+1}, \tag{9}$$

$$\frac{R_{n+1}-R_n}{\phi(h)} = \gamma I_{n+1} - \mu R_{n+1}. \tag{10}$$

Let total population $N_n = S_n + I_n + R_n$, adding three equations (7), (8) and (10), we can see that the conservation law holds:

$$\frac{N_{n+1}-N_n}{\phi(h)} = \Lambda - \mu N_{n+1} - u_1 I_{n+1} \leq \Lambda - \mu N_{n+1}. \tag{11}$$

Based on Micken's work ([24]), the denominator function can be calculated $\phi(h) = \frac{e^{\mu h}-1}{\mu}$. Since equations (7-10) are linear in S_{n+1}, I_{n+1}, B_{n+1} and R_{n+1}, we obtain their explicit version after rearranging:

$$S_{n+1} = \frac{S_n + \Lambda\phi(h)}{1+\phi(h)(\mu+\Phi(I_n,B_n))}, \tag{12}$$

$$I_{n+1} = \frac{I_n + \phi(h)S_{n+1}\Phi(I_n,B_n)}{1+\phi(h)(\gamma+\mu+u_1)}, \tag{13}$$

$$B_{n+1} = \frac{B_n + \xi\phi(h)I_{n+1}}{1+\delta\phi(h)}, \tag{14}$$

$$R_{n+1} = \frac{R_n + \gamma\phi(h)I_{n+1}}{1+\mu\phi(h)}, \tag{15}$$

for the convenience of calculations, we set $\Phi(I_n, B_n) = \beta_h I_n + \frac{\beta_e B_n}{\kappa + B_n}$. Moreover, the following theorems can show the positivity and boundedness:

Theorem 3.1. *If all the initial values and the parameter values of the discrete system* (12)-(15) *are positive, then the numerical solutions are always positive for all* $n \geq 0$*, all denominator function* $\phi(h)$*.*

Theorem 3.2. *The NSFD scheme defines the discrete dynamical system* (12)-(15) *on the following biologically feasible invariant region*:

$$\tilde{D} = \{(S_n, I_n, R_n) \,|\, S_n \geq 0, I_n \geq 0, R_n \geq 0, S_n + I_n + R_n \leq \frac{\Lambda}{\mu}\}, n = 0, 1, 2, \ldots$$

4. Stability of the disease-free equilibrium

In order to study the convergence of the scheme (12)-(15), it is enough to only consider equations (12)-(14). The continuous and discrete models have the same equilibria, we first discuss the stability of proposed NSFD numerical scheme at the disease-free equilibrium $\tilde{E}_0 = (S(0), I(0), R(0))$.

First, we present the following Lemma ([7]):

Lemma 4.1 ([7])**.** *For the quadratic equation* $\lambda^2 - a\lambda + b$*, both roots satisfy* $|\lambda_i| < 1$*,* $i = 1, 2$*, if and only if the following conditions are satisfied*:

(1) $f(0) = b < 1$;

(2) $f(-1) = 1 + a + b > 0$;
(3) $f(1) = 1 - a + b > 0$.

First of all, let us consider the linearization of system (12-14) at the DFE point $\tilde{E}_0$. Let $\gamma + \mu + u_1 = Q$, the Jacobian matrix for the model system is:

$$\begin{bmatrix} \frac{1}{1+\mu\phi(h)} & \frac{-(\frac{\Lambda}{\mu}+\Lambda\phi(h))\beta_h\phi(h)}{(1+\mu\phi(h))^2} & \frac{-(\frac{\Lambda}{\mu}+\Lambda\phi(h))\beta_e\phi(h)}{\kappa(1+\mu\phi(h))^2} \\ 0 & \frac{1}{1+Q\phi(h)}(1+\frac{(\frac{\Lambda}{\mu}+\Lambda\phi(h))\beta_h\phi(h)}{1+\mu\phi(h)}) & \frac{(\frac{\Lambda}{\mu}+\Lambda\phi(h))\beta_e\phi(h)}{\kappa(1+\mu\phi(h))(1+Q\phi(h))} \\ 0 & \frac{\xi\phi(h)}{1+\delta\phi(h)}[\frac{1}{1+Q\phi(h)}(1+\frac{(\frac{\Lambda}{\mu}+\Lambda\phi(h))\beta_h\phi(h)}{1+\mu\phi(h)})] & \frac{1}{1+\delta\phi(h)}+\frac{\xi\phi(h)}{1+\delta\phi(h)}[\frac{(\frac{\Lambda}{\mu}+\Lambda\phi(h))\beta_e\phi(h)}{\kappa(1+\mu\phi(h))(1+Q\phi(h))}] \end{bmatrix}.$$

The characteristic polynomial at the DFE $\tilde{E}_0$ is found as:

$$(\lambda - \frac{1}{1+\mu\phi(h)})(\lambda^2 - a\lambda + b) = 0, \tag{16}$$

where

$$\begin{aligned} a &= \frac{1}{1+\delta\phi(h)} + \frac{\xi\beta_e\phi(h)^2(\frac{\Lambda}{\mu}+\Lambda\phi(h))}{\kappa(1+Q\phi(h))(1+\mu\phi(h))(1+\delta\phi(h))} + \frac{1}{1+Q\phi(h)} \\ &\quad + \frac{\beta_h\phi(h)(\frac{\Lambda}{\mu}+\Lambda\phi(h))}{(1+\mu\phi(h))(1+Q\phi(h))}, \\ b &= \frac{1}{(1+Q\phi(h))(1+\delta\phi(h))} + \frac{\beta_h\phi(h)(\frac{\Lambda}{\mu}+\Lambda\phi(h))}{(1+\mu\phi(h))(1+Q\phi(h))(1+\delta\phi(h))}. \end{aligned}$$

Obviously, the first root $\lambda_1 = \frac{1}{1+\mu\phi(h)}$ is less than 1. Next, in order to compute the other two eigenvalues, we define $f(\lambda) = \lambda^2 - a\lambda + b$. Among the three conditions in Lemma 4.1, the second one is obvious since $a > 0$ and $b > 0$. To show $f(0) < 1$, it is need to prove that

$$1 + \mu\phi(h) + \beta_h\phi(h)(\frac{\Lambda}{\mu} + \Lambda\phi(h)) < (1+\phi(h))(1+\delta\phi(h))(1+\mu\phi(h)),$$

which is then equivalent to

$$\begin{aligned} &\frac{\Lambda\phi(h)\beta_h}{\mu} + \Lambda\beta_h\phi(h)^2 \\ &< \delta\phi(h) + Q\phi(h) + \mu\delta\phi(h)^2 + \mu Q\phi(h)^2 + \delta Q\phi(h)^2 + \mu\delta Q\phi(h)^3. \end{aligned}$$

Meanwhile, $R_0 < 1$ yields $\Lambda\kappa\beta_h < \mu Q$. Now we use the facts that $\frac{\Lambda\phi(h)\beta_h}{\mu} < Q\phi(h)$ and $\Lambda\phi(h)^2\beta_h < \mu Q\phi(h)^2$, it is easy to calculate that $f(0) < 1$ holds. For the condition (3), we note

$$\begin{aligned} f(1) &= \frac{\delta\phi(h)}{1+\delta\phi(h)} + \frac{1}{(1+\delta\phi(h))(1+Q\phi(h))} \\ &\quad + \frac{\phi(h)(\frac{\Lambda}{\mu}+\Lambda\phi(h))[\beta_h - \xi\frac{\phi(h)\beta_e}{\kappa} - \beta_h(1+\delta\phi(h))]}{(1+\delta\phi(h))(1+Q\phi(h))(1+\mu\phi(h))} \end{aligned}$$

$$
\begin{aligned}
&= \frac{\delta Q\phi(h)^2}{(1+\delta\phi(h))(1+Q\phi(h))} - \frac{\phi(h)^2(\frac{1}{\mu}+\phi(h))(\frac{\Lambda\xi\beta_e}{\kappa}+\Lambda\beta_h\delta)}{(1+\delta\phi(h))(1+Q\phi(h))(1+\mu\phi(h))} \\
&> \frac{\delta Q\phi(h)^2}{(1+\delta\phi(h))(1+Q\phi(h))} - \frac{\phi(h)^2(\frac{1}{\mu}+\phi(h))\mu\delta Q}{(1+\delta\phi(h))(1+Q\phi(h))(1+\mu\phi(h))} \\
&> 0.
\end{aligned}
$$

Therefore, all conditions in Lemma 4.1 are satisfied if $R_0 < 1$ and ensure the asymptotic stability of $\tilde{E}_0$.

Thus, we establish the following result:

Theorem 4.2. *The disease-free equilibrium of the discrete model* (12)-(14) *is locally asymptotically stable if* $R_0 < 1$.

Next, we will analyze the global stability at the DFE of the discrete system.

Theorem 4.3. *The disease-free equilibrium of the discrete model* (12)-(14) *is globally asymptotically stable if* $R_0 < 1$.

Proof. For any $\epsilon > 0$, there exists an integer n_0, for any $n \geq n_0$ such that

$$S_{n+1} \leq \frac{\Lambda}{\mu} + \epsilon. \tag{17}$$

Consider the following sequence $\{V(n)\}_{n=0}^{+\infty}$:

$$V(n) = I_n + \frac{\gamma+\mu+u_1}{\xi}B_n + \phi\beta_h S_{n+1}I_n + \phi\beta_e\frac{S_{n+1}B_n}{\kappa+B_n}. \tag{18}$$

For any $n \geq n_0$, the difference of $V(n)$ satisfies

$$
\begin{aligned}
&V(n+1) - V(n) \\
&= I_{n+1} + \frac{\gamma+\mu+u_1}{\xi}B_{n+1} + \phi\beta_h S_{n+2}I_{n+1} + \phi\beta_e\frac{S_{n+2}B_{n+1}}{\kappa+B_{n+1}} - I_n \\
&\quad - \frac{\gamma+\mu+u_1}{\xi}B_n - \phi\beta_h S_{n+1}I_n - \phi\beta_e\frac{S_{n+1}B_n}{\kappa+B_n} \\
&= \phi\beta_e\frac{S_{n+1}B_n}{\kappa+B_n} + \phi\beta_h S_{n+1}I_n - \phi(\gamma+\mu+u_1)I_{n+1} + \phi(\gamma+\mu+u_1)I_{n+1} \\
&\quad - \frac{\gamma+\mu+u_1}{\xi}\delta\varphi B_{n+1} + \phi\beta_h S_{n+2}I_{n+1} + \phi\beta_e\frac{S_{n+2}B_{n+1}}{\kappa+B_{n+1}} \\
&= \phi\beta_h S_{n+2}I_{n+1} + \phi\beta_e\frac{S_{n+2}B_{n+1}}{\kappa+B_{n+1}} - \frac{\gamma+\mu+u_1}{\xi}\delta\phi B_{n+1} \\
&\leq \phi\frac{\Lambda}{\mu}(\beta_h I_{n+1} + \frac{\beta_e\xi I_{n+1}}{\delta\kappa}) - (\gamma+\mu+u_1)\phi I_{n+1} \\
&= \phi I_{n+1}(\gamma+\mu+u_1)(R_0-1).
\end{aligned}
$$

Since ε is arbitrary, for any $n \geq 0$, we conclude $V(n+1) - V(n) \leq 0$ and $\lim_{n\to\infty} I_n = 0$ if $R_0 < 1$. The sequence $\{V(n)\}_{n=0}^{+\infty}$ is a monotone decreasing sequence, meanwhile, $\lim_{n\to\infty} S_n = \frac{\Lambda}{\mu}$. This completes the proof. □

5. Stability of the endemic equilibrium

In this section, we study the local stability of the endemic equilibrium $\tilde{E^*} = (S^*, I^*, B^*, R^*)$ of the discrete system. After setting the right hand sides of equations (7)-(10) equal to zero, one can find that the equilibrium points of the NSFD scheme are the same as those obtained for the original continuous model.

Theorem 5.1. *The endemic equilibrium of the discrete model is globally asymptotically stable if* $R_0 > 1$.

Proof. We construct a sequence $\{\tilde{V}(n)\}_{n=1}^{+\infty}$ of the form,

$$\tilde{V}(n) = \frac{1}{\phi\beta_h I^*} g(\frac{S_n}{S^*}) + \frac{1}{\phi\beta_h S^*} g(\frac{I_n}{I^*}) + \frac{\beta_e}{\phi\beta_h \delta I^*} g(\frac{B_n}{B^*}), \tag{19}$$

where the function $g(x) = x - 1 - \ln x$, $x \in R^+$, clearly, $g(x) \geq 0$ with equality only if $x = 1$. First, we have

$$\begin{aligned}
& g(\frac{S_{n+1}}{S^*}) - g(\frac{S_n}{S^*}) = \frac{S_{n+1}}{S^*} - \frac{S_n}{S^*} - \ln\frac{S_{n+1}}{S_n} \\
\leq\ & \frac{S_{n+1} - S_n}{S^*} - \frac{S_{n+1} - S_n}{S_{n+1}} \\
=\ & \frac{S_{n+1} - S^*}{S^* S_{n+1}}(S_{n+1} - S_n) \\
=\ & \frac{S_{n+1} - S^*}{S^* S_{n+1}}\phi(\Lambda - \beta_e \frac{S_{n+1}B_n}{\kappa + B_n} - \beta_h S_{n+1} I_n - \mu S_{n+1}) \\
=\ & \frac{S_{n+1} - S^*}{S^* S_{n+1}}\phi(\beta_e \frac{S^* B^*}{\kappa + B^*} + \beta_h S^* I^* + \mu S^* - \beta_e \frac{S_{n+1}B_n}{\kappa + B_n} - \beta_h S_{n+1} I_n - \mu S_{n+1}) \\
=\ & -\frac{\mu\phi(S_{n+1} - S^*)^2}{S^* S_{n+1}} + \phi\beta_h I^*(1 - \frac{S^*}{S_{n+1}})(1 - \frac{S_{n+1} I_n}{S^* I^*}) \\
& + \frac{\beta_e \phi B^*}{\kappa + B^*}(1 - \frac{S^*}{S_{n+1}})(1 - \frac{S_{n+1}B_n}{\kappa + B_n}\frac{\kappa + B^*}{S^* B^*}).
\end{aligned}$$

In the same way, we have

$$\begin{aligned}
& g(\frac{I_{n+1}}{I^*}) - g(\frac{I_n}{I^*}) = \frac{I_{n+1}}{I^*} - \frac{I_n}{I^*} - \ln\frac{I_{n+1}}{I_n} \\
\leq\ & \frac{I_{n+1} - I_n}{I^*} - \frac{I_{n+1} - I_n}{I_{n+1}} \\
=\ & \frac{I_{n+1} - I^*}{I^* I_{n+1}}(I_{n+1} - I_n) \\
=\ & \frac{I_{n+1} - I^*}{I^* I_{n+1}}\phi[\beta_e \frac{S_{n+1}B_n}{\kappa + B_n} + \beta_h S_{n+1} I_n - (\gamma + \mu + u_1) I_{n+1}] \\
=\ & \frac{I_{n+1} - I^*}{I^* I_{n+1}}\phi[\beta_e \frac{S_{n+1}B_n}{\kappa + B_n} + \beta_h S_{n+1} I_n - \frac{\beta_e I_{n+1} S^* B^*}{(\kappa + B^*) I^*} - \beta_h I_{n+1} S^*]
\end{aligned}$$

$$= \phi\beta_h S^*(1-\frac{I^*}{I_{n+1}})(\frac{S_{n+1}}{S^*}\frac{I_n}{I^*}-\frac{I_{n+1}}{I^*}) + \frac{\phi\beta_e}{I^*}(1-\frac{I^*}{I_{n+1}})[\frac{S_{n+1}B_n}{\kappa+B_n}-\frac{I_{n+1}S^*B^*}{(\kappa+B^*)I^*}].$$

Similarly, by letting $\xi I^* = \delta W^*$, we obtain

$$\begin{aligned} & g(\frac{B_{n+1}}{B^*}) - g(\frac{B_n}{B^*}) \\ = & \frac{B_{n+1}}{B^*} - \frac{B_n}{B^*} - \ln\frac{B_{n+1}}{B_n} \\ \le & \frac{B_{n+1}-B^*}{B^*B_{n+1}}(B_{n+1}-B_n) \\ = & \frac{B_{n+1}-B^*}{B^*B_{n+1}}\phi(\xi I_{n+1}-\delta B_{n+1}) \\ = & \frac{\delta\phi}{B^*}(1-\frac{B^*}{B_{n+1}})(\frac{B^*}{I^*}I_{n+1}-B_{n+1}). \end{aligned}$$

The difference of $\tilde{V}(n)$ satisfies,

$$\begin{aligned} & \tilde{V}(n+1)-\tilde{V}(n) \\ = & \frac{1}{\phi\beta_h I^*}[\frac{S_{n+1}-S_n}{S^*}+\ln(\frac{S_n}{S_{n+1}})] + \frac{1}{\phi\beta_h S^*}[\frac{I_{n+1}-I_n}{I^*}+\ln(\frac{I_n}{I_{n+1}})] \\ & + \frac{\beta_e}{\phi\beta_h\delta I^*}[\frac{B_{n+1}-B_n}{B^*}+\ln(\frac{B_n}{B_{n+1}})] \\ \le & -\frac{\mu(S_{n+1}-S^*)^2}{\beta_h S_{n+1}S^*I^*} + (-\frac{S^*}{S_{n+1}}-\frac{I_{n+1}}{I^*}-\frac{S_{n+1}I_n}{I_{n+1}S^*}+\frac{I_n}{I^*}+2) - \frac{\beta_e}{\beta_h I^*}\frac{B^*}{\kappa+B^*} \\ & (\frac{S^*}{S_{n+1}}+\frac{I_{n+1}}{I^*}+\frac{I^*S_{n+1}B_n}{I_{n+1}(\kappa+B_n)S^*}\frac{\kappa+B^*}{B^*}-\frac{B_n}{\kappa+B_n}\frac{\kappa+B^*}{B^*}-2) \\ & -\frac{\beta_e}{\beta_h I^*}\frac{B^*}{\kappa+B^*}(\frac{B_{n+1}}{B^*}+\frac{B^*I_{n+1}}{B_{n+1}I^*}-\frac{I_{n+1}}{I^*}-1) \\ \le & -\frac{\mu(S_{n+1}-S^*)^2}{\beta_h S_{n+1}S^*I^*} - [g(\frac{S^*}{S_{n+1}})+g(\frac{S_{n+1}I_n}{I_{n+1}S^*})+\frac{I_{n+1}}{I^*}-\ln\frac{I_{n+1}}{I_n}] \\ & -\frac{\beta_e}{\beta_h I^*}\frac{B^*}{\kappa+B^*}(\frac{S^*}{S_{n+1}}+\frac{I_{n+1}}{I^*}+\frac{I^*S_{n+1}}{S^*I_{n+1}}\frac{\kappa+B^*}{B^*}-\frac{\kappa+B^*}{B^*}-2) \\ & -\frac{\beta_e}{\beta_h I^*}\frac{B^*}{\kappa+B^*}(\frac{B_{n+1}}{B^*}+\frac{B^*I_{n+1}}{B_{n+1}I^*}-\frac{I_{n+1}}{I^*}-1) \\ \le & -\frac{\mu(S_{n+1}-S^*)^2}{\beta_h S_{n+1}S^*I^*} - g(\frac{S^*}{S_{n+1}}) - g(\frac{S^*}{S_{n+1}}) - g(\frac{S_{n+1}I_n}{I_{n+1}S^*}) - \frac{\beta_e}{\beta_h I^*}\frac{B^*}{\kappa+B^*} \\ & [g(\frac{S^*}{S_{n+1}})+g(\frac{I_{n+1}S_{n+1}}{I_{n+1}S^*}\frac{\kappa+B^*}{B^*})+g(\frac{B_{n+1}}{B^*})+g(\frac{B^*I_{n+1}}{B_{n+1}I^*})]. \end{aligned}$$

Therefore, for any $n \geq 0$, $\{\tilde{V}(n)\}$ is a monotone decreasing sequence. Since $\tilde{V}(n) > 0$, $\lim_{n\to\infty}(\tilde{V}(n+1) - \tilde{V}(n)) = 0$, we then obtain $\lim_{n\to} S_{n+1} = S^*$, $\lim_{n\to\infty} I_{n+1} = I^*$ as well as $\lim_{n\to\infty} R_{n+1} = R^*$. This completes the proof. □

6. Numerical results

In this section, numerical simulations are proposed to exam convergence and stability properties of the NSFD scheme.

We use the data regarding the course of the cholera in Zimbabwe for the period from August 2008 to July 2009. The Zimbabwean cholera outbreak not only swept to all of Zimbabwe's ten provinces but also spread quickly to Botswana, Mozambique, South Africa and Zambia. This epidemic has been treated as the Africa's worst outbreak over the last 15 years with high death rate, killed more than 4,300 people and infected over 100,000. The total population in Zimbabwe is 12,347,240, in order to match the hypothetical population of $N = 10,000$ in [29] and make the calculation simpler, we scale down all data numbers by a factor of 1,200, the initial values are taken as $S(0) = 9999$, $I(0) = 1$, $B(0) = 0$, and $R(0) = 0$ according to the data published by WHO. All epidemiological parameter values for cholera in literature are given in Table 1. The discussions in ([14, 29]) indicated that parameters β_e and β_h are sensitive and vary from place to place, therefore, these two parameters are modified in the numerical simulations as $\beta_e = 0.075$, $\beta_h = 0.00011$ to match the real reported infections in Zimbabwe.

To investigate the stability of the equilibria for our discrete model (11)-(14) numerically, we perform several numerical simulations of the NSFD scheme and compare the results with other well-known schemes such as Euler's method and the fourth-order Runge-Kutta (RK4) method to find out when numerical instabilities appear for each scheme. Parameters used for this part of the simulations are taken from Table 1, which give $R_0 > 1$ and the endemic equilibrium is $(0.5135, 7848.0744, 2151.4121)$ by calculation. In Table 2, the spectral radius ρ of the Jacobian of the NSFD scheme evaluated at the endemic equilibrium point is presented and compared with that of Euler and RK4 methods from

TABLE 1. model parameters and values.

Parameter	Symbol	Value	Source
the natural human death rate	μ	$(35y)^{-1}$	[40]
the disease-related death rate	u_1	0.0015	[28]
recruitment rate of susceptible population	Λ	4.5	Assumed
concentration of vibrios in water	κ	1000000	[10, 14]
the shedding rate	ξ	70	[14, 28]
the bacterial death rate	δ	$(30d)^{-1}$	[14]
rate of recovery from cholera	γ	$(5d)^{-1}$	[14]

TABLE 2. Qualitative results for different schemes with different time step sizes h when $R_0 > 1$.

h	ρ-Euler	ρ-RK4	ρ-NSFD
0.01	0.9995-Convergence	0.9999-Convergence	0.9999-Convergence
0.1	0.9994-Convergence	0.9999-Convergence	0.9999-Convergence
0.5	0.9994-Convergence	0.9995-Convergence	0.9995-Convergence
1	0.9992-Convergence	0.9990-Convergence	0.9994-Convergence
2	1.3729-Divergence	0.9990-Convergence	0.9993-Convergence
5	Divergence	0.9789-Convergence	0.9893-Convergence
8	Divergence	0.9384-Convergence	0.9800-Convergence
9	Divergence	1.0034-Divergence	0.9875-Convergence
15	Divergence	Divergence	0.9801-Convergence
20	Divergence	Divergence	0.9729-Convergence
25	Divergence	Divergence	0.9637-Convergence
30	Divergence	Divergence	0.9699-Convergence

TABLE 3. Qualitative results of NSFD scheme for different time step sizes h and different initial conditions when $R_0 > 1$.

h	$I(0)$	$S(0)$	$R(0)$	$B(0)$	ρ-NSFD
1	1	9999	0	0	0.9994-Convergence
1	100	9900	0	0	0.9997-Convergence
1	1000	9000	0	0	0.9996-Convergence
10	1	9999	0	0	0.9996-Convergence
10	100	9900	0	0	0.9971-Convergence
10	1000	9000	0	0	0.9970-Convergence
20	1	9999	0	0	0.9729-Convergence
20	100	9900	0	0	0.9843-Convergence
20	1000	9000	0	0	0.9772-Convergence

$h = 0.01$ to $h = 30$. It is obvious to see that the Euler method is the first to fail for a time step size of $h = 2$, the RK4 behaves better for smaller h but fails when $h \geq 21$. However, scheme NSFD converges for any time step sizes in the numerical simulations. Table 3 depicts the convergence property of the NSFD scheme with several sets of initial conditions and step sizes. As it can be observed, the spectral radius of Jacobian matrix associated to NSFD scheme evaluated at the endemic equilibrium point are less than one all the time, which shows not only the stability of the endemic equilibrium, but also the NSFD scheme is more competitive in terms of numerical stability. In another case, we adjust the key parameters $\beta_e = 0.05$ and $\beta_h = 0.00005$ to set $R_0 = 0.47$, we simulate qualitative convergence results for various time step sizes and different initial conditions in Table 4, the results confirm our theoretical work in Section 4.

TABLE 4. Qualitative results of NSFD scheme for different time step sizes h and different initial conditions when $R_0 < 1$.

h	$I(0)$	$S(0)$	$R(0)$	$B(0)$	ρ-NSFD
1	1	9999	0	0	0.9999-Convergence
1	100	9900	0	0	0.9999-Convergence
1	1000	9000	0	0	0.9996-Convergence
10	1	9999	0	0	0.9999-Convergence
10	100	9900	0	0	0.9921-Convergence
10	1000	9000	0	0	0.9883-Convergence
20	1	9999	0	0	0.9863-Convergence
20	100	9900	0	0	0.9614-Convergence
20	1000	9000	0	0	0.9755-Convergence

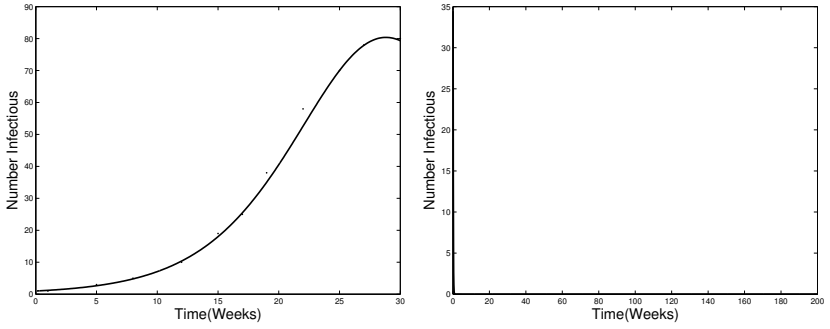

(a) (b)

FIGURE 1. (a) The phase plane portrait of I vs. Time (weeks) for $R_0 > 1$ with $h = 1$, shows data fitting for the cholera outbreak in Zimbabwe, where the curve represents the model prediction and the points mark the reported data from WHO. Initial conditions are $I(0) = 1$, $S(0) = 9999$, and $B(0) = R(0) = 0$; (b) The phase plane portrait of I vs. Time (weeks) for $R_0 < 1$ with $h = 1$. Initial conditions are $I(0) = 1$, $S(0) = 9999$, and $B(0) = R(0) = 0$.

With $h = 1$, one can see from Fig. 1(a) that cholera outbreak increases rapidly from the initial day and reaches the peak at $t = 30$ weeks with value 80 (normalized value), which fits well the real data in Zimbabwe. To predict the cholera epidemic for a long time, we run the numerical simulation until $t = 20,000$ weeks. The first highest point 80 in Fig. 2(a) shows the 2008-2009 cholera outbreak, it then starts to gradually drop to almost zero, meaning the disease is gradually eradicated from the population, after the first peak, several

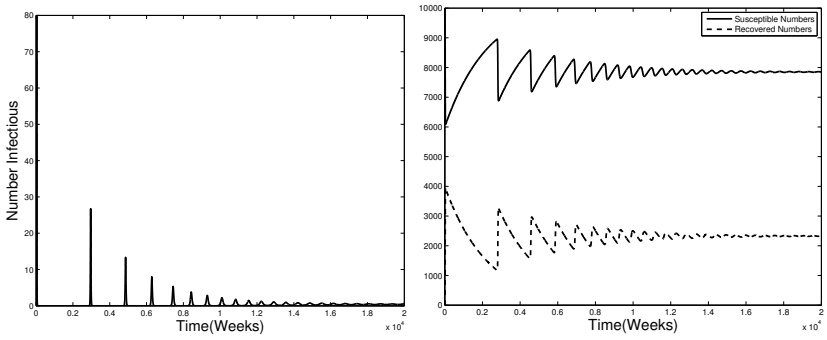

(a) (b)

FIGURE 2. (a) The phase plane portrait of I vs. Time (weeks) with $h = 1$ until $t = 20,000$ weeks; (b) The phase plane portrait of S and R vs. Time (weeks) with $h = 1$ until $t = 20,000$ weeks.

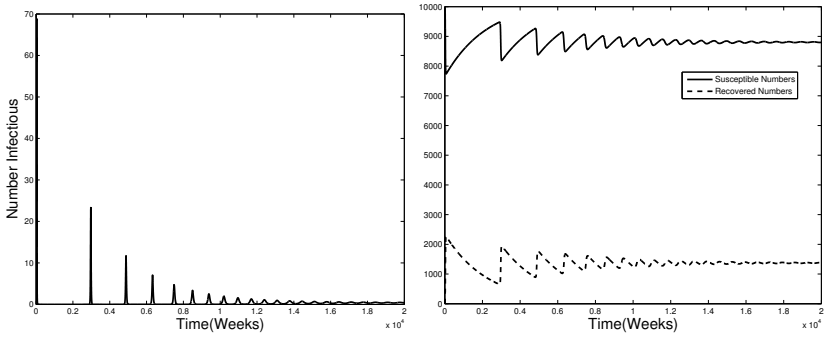

(a) (b)

FIGURE 3. (a) The phase plane portrait of I vs. Time (weeks) with $h = 9$ until $t = 20,000$ weeks. Initial conditions are $I(0) = 1$, $S(0) = 9999$, and $B(0) = R(0) = 0$; (b) The phase plane portrait of S and R vs. Time (weeks) with $h = 9$ until $t = 20,000$ weeks.

oscillations appear later with smaller and smaller peak values, representing cholera will restart again and again and the total extinction of cholera after $t = 20,000$ weeks. Fig. 2(b) shows almost the same trend with different magnitude for susceptible population S and recovered population R. On the other hand, we set the key parameters β_e and β_h as 0.05 and 0.00005 to make $R_0 < 1$, as shown in Fig. 1(b), the disease dies out quickly, so that it can be eradicated.

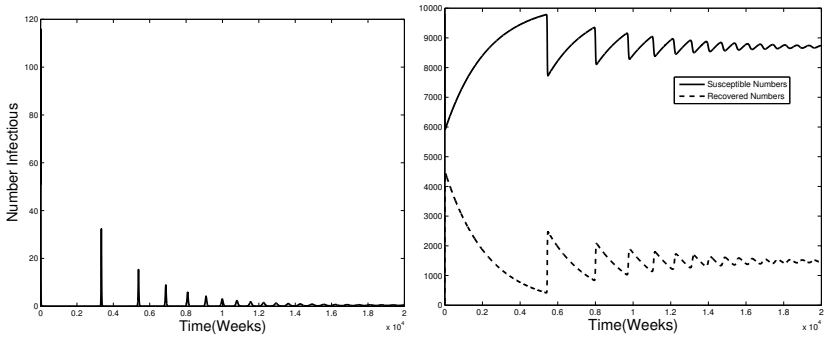

(a) (b)

FIGURE 4. (a) The phase plane portrait of I vs. Time (weeks) with $h = 1$ until $t = 20,000$ weeks. Initial conditions are $I(0) = 500$, $S(0) = 9500$, and $B(0) = R(0) = 0$; (b) The phase plane portrait of S and R vs. Time (weeks) with $h = 1$ until $t = 20,000$ weeks. Initial conditions are $I(0) = 500$, $S(0) = 9500$, and $B(0) = R(0) = 0$.

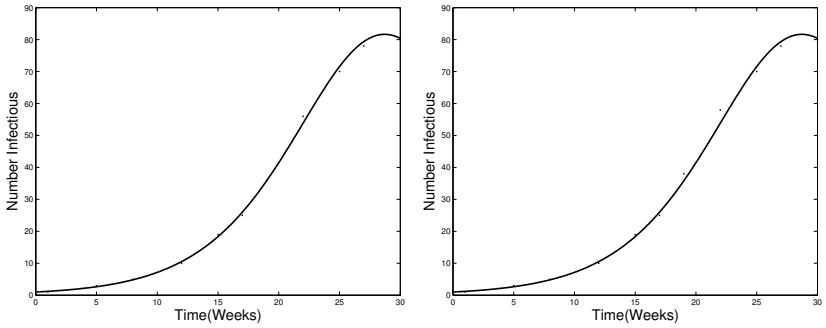

(a) (b)

FIGURE 5. (a) The phase plane portrait of I vs. Time (weeks) for the Euler scheme with $h = 1$; (b) The phase plane portrait of I vs. Time (weeks) for the RK4 scheme with $h = 1$.

When we take $h = 9$, it can be seen that all three subpopulations evolve asymptotically to their steady states in Fig. 3, this pattern is also observed with other time step sizes, which demonstrates the convergence of NSFD scheme to the endemic equilibrium points is irrespective of the time step sizes. We present numerical simulations in Fig. 4 until $t = 20,000$ weeks with different

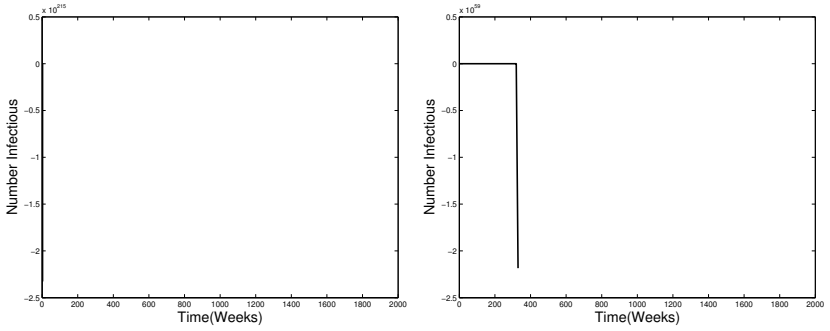

(a) (b)

FIGURE 6. (a) The phase plane portrait of I vs. Time (weeks) for the Euler scheme with $h = 2$; (b) The phase plane portrait of I vs. Time (weeks) for the RK4 scheme with $h = 9$.

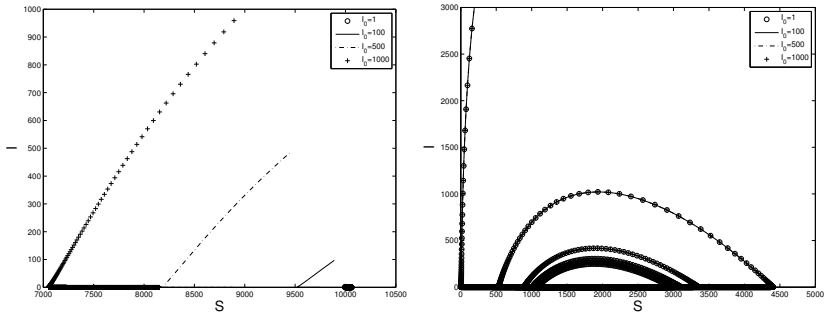

(a) (b)

FIGURE 7. (a) The phase plane portrait of I vs. S for $R_0 < 1$, all these orbits converge to the disease-free equilibrium $\tilde{E}_0$; (b) The phase plane portrait of I vs. S for $R_0 > 1$, all these orbits converge to the endemic equilibrium $\tilde{E}^*$.

initial conditions: $I(0) = 500$, $S(0) = 9500$, and $B(0) = R(0) = 0$, very similar pattern is observed.

Fig. 5(a) and (b) show how the Euler and RK4 schemes converge to their equilibria with $h = 1$, respectively. However, when the step size is increased further, Fig. 6(a) and (b) show that the Euler scheme and RK4 scheme fail to converge using a step-size of length $h = 2$ and $h = 9$, respectively.

At last, to verify the global asymptotic stability of the NSFD scheme analyzed in Section 4 and Section 5, we pick four different initial conditions with

$I(0) = 1, 100, 500, 1000$, respectively, and plot these four solution curves by the phase plane portrait of I vs. S. It is clearly that all these four orbits converge to the disease-free equilibrium $\tilde{E}_0$ when $R_0 < 1$ in Fig. 7(a) and converge to endemic equilibrium $\tilde{E^*}$ when $R_0 > 1$ in Fig. 7(b), respectively.

7. Conclusions and discussions

Until now, a lot of continuous cholera models have been formulated and analyzed, nevertheless, the discrete cholera models are quite few. In the present paper, an NSFD numerical scheme is proposed for solving mathematical cholera model and its asymptotical behaviors are studied. The discrete system (11)-(14) is dynamically consistent with its continuous model (1)-(4), it preserves essential properties, such as positivity, conservation law and the boundedness of the solution, equilibrium points as well as their stability properties. In particular, the main contribution of this paper is that we have established a complete analysis of the global stability of the disease-free and endemic equilibria by applying the techniques of Lyapunov functions.

At last, we applied the discrete model to study the transmission of cholera in Zimbabwe (2008-2009). We have carried out numerical simulations and concluded that the stability and convergence properties of the NSFD scheme are irrespective of the time step sizes. Further, we have showed that NSFD scheme is stable and converge to the disease-free equilibrium point for $R_0 < 1$, and it is also convergent to the endemic equilibrium point based on the numerical simulation. In addition, we showed numerical advantages of the NSFD scheme compared with Euler's scheme and the RK4 scheme for various time step sizes. Euler scheme and RK4 scheme diverge when $h > 2$ and $h > 9$ whereas NSFD scheme does not. Therefore, when we study cholera, the statistic data was collected weekly (from WHO), it is more direct and convenient to simulate the disease better than using the continuous-time model. Furthermore, larger time step size can be use to save the computational time and memory. In a word, our results suggest that the NSFD scheme outperforms the traditional schemes.

It is a pity that we didn't prove the local stability of endemic equilibrium analytically for the case $R_0 > 1$ because the calculation is tedious, we plan to pursue it on a separate paper.

Acknowledgment. The authors are grateful to the anonymous reviewers for constructive suggestions and valuable comments, which improve the quality of the article.

References

[1] L. Allen, *Some discrete-time SI, SIR, and SIS epidemic models*, Math. Biosci. **124** (1994), no. 1, 83–105.

[2] L. Allen and A. Burgin, *Comparison of deterministic and stochastic SIS and SIR models in discrete time*, Math. Biosci. **63** (2000), no. 1, 1–33.

[3] L. Allen, D. Flores, R. Ratnayake, and J. Herbold, *Discrete-time deterministic and stochastic models for the spread of rabies*, Appl. Math. Comput. **132** (2002), no. 2-3, 271–292.
[4] R. Anguelov and J. M. S. Lubuma, *Contributions to the mathematics of the nonstandard finite difference method and applications*, Numer. Methods Partial Differential Equations **17** (2001), no. 5, 518–543.
[5] ———, *Nonstandard finite difference method by nonlocal approximation*, Math. Comput. Simulation **61** (2003), no. 3-6, 465–475.
[6] A. J. Arenas, G. Gonzalez-Parra, and B. M. Chen-Charpentier, *A nonstandard numerical scheme of predictor-corrector type for epidemic models*, Comput. Math. Appl. **59** (2010), no. 12, 3740–3749.
[7] F. Brauer and C. Castillo-Chavez, *Mathematical Models in Population Biology and Epidemiology*, Springer, New York, NY, 2001.
[8] V. Capasso and S. L. Paveri-Fontana, *A mathematical model for the 1973 cholera epidemic in the European Mediterranean region*, Rev Epidemiol Sante Publique **27** (1979), 121–132.
[9] C. Castillo-Chavez and A. A. Yakubu, *Discrete-time SIS models with complex dynamics*, Nonlinear Anal. **47** (2001), no. 7, 4753–4762.
[10] C. T. Codeço, *Endemic and epidemic dynamics of cholera: the role of the aquatic reservoir*, BMC Infectious Diseases (2001), 1.1.
[11] S. M. Garba, A. B. Gumel, and J. M. S. Lubuma, *Dynamically-consistent non-standard finite difference method for an epidemic model*, Math. Comput. Modelling **53** (2011), no. 1-2, 131–150.
[12] F. Guerrero, G. Gonzalez-Parra, and A. J. Arenas, *A nonstandard finite difference numerical scheme applied to a mathematical model of the prevalence of smoking in Spain: a case study*, Comput. Appl. Math. **33** (2013), no. 1, 1–13.
[13] A. B. Gumel, C. Connell McCluskey, and J. Watmough, *An SVEIR model for assessing potential impact of an imperfect anti-SARS vaccine*, Math. Biosci. Eng. **3** (2006), no. 3, 485–512.
[14] D. M. Hartley, J. G. Morris, and D. L. Smith, *Hyperinfectivity: A critical element in the ability of V. cholerae to cause epidemics?*, PLoS Medicine **3** (2006), 63–69.
[15] S. D. Hove-Musekwa, F. Nyabadza, C. Chiyaka, P. Das, A. Tripathi, and Z. Mukandavire, *Modelling and analysis of the effects of malnutrition in the spread of cholera*, Math. Comput. Modelling **53** (2011), no. 9-10, 1583–1595.
[16] Z. Hu, Z. Teng, and H. Jiang, *Stability analysis in a class of discrete SIRS epidemic models*, Nonlinear Anal. Real World Appl. **13** (2012), no. 5, 2017–2033.
[17] Z. Hu, Z. Teng, and L. Zhang, *Stability and bifurcation analysis in a discrete SIR epidemic model*, Math. Comput. Simulation **97** (2014), no. 2, 80–93.
[18] L. Jodar, R. J. Villanueva, A. J. Arenas, and G. C. Gonzalez, *Nonstandard numerical methods for a mathematical model for influenza disease*, Math. Comput. Simulation **79** (2008), no. 3, 622–633.
[19] S. Liao and J. Wang, *Stability analysis and application of a mathematical cholera model*, Math. Biosci. Eng. **8** (2011), no. 3, 733–752.
[20] S. Liao and W. Yang, *On the dynamics of a vaccination model with multiple transmission way*, Int. J. Appl. Math. Comput. Sci. **23** (2013), no. 4, 761–772.
[21] X. Ma, Y. Zhou, and H. Cao, *Global stability of the endemic equilibrium of a discrete SIR epidemic model*, Adv. Difference Equ. **2013** (2013), 19 pp.
[22] R. E. Mickens, *Exact solutions to a finite difference model of a nonlinear reaction-advection equation: implications for numerical analysis*, Numer. Methods Partial Differential Equations **5** (1989), no. 4, 313–325.
[23] ———, *Nonstandard Finite Difference Models of Differential Equations*, World Scientific, Singapore, 1994.

[24] ———, *Dynamic consistency: a fundamental principle for constructing nonstandard finite difference schemes for differential equations*, J. Difference Equ. Appl. **11** (2005), no. 7, 645–653.
[25] ———, *Calculation of denominator functions for nonstandard finite difference schemes for differential equations satisfying a positivity condition*, Wiley Inter. Sci. **23** (2006), no. 3, 672–691.
[26] ———, *Discretizations of nonlinear differential equations using explicit nonstandard methods*, J. Comput. Appl. Math. **110** (1999), no. 1, 181–185.
[27] A. K. Misra and V. Singh, *A delay mathematical model for the spread and control of water borne diseases*, J. Theoret. Biol. **301** (2012), 49–56.
[28] Z. Mukandavire and W. Garira, *Sex-structured HIV/AIDS model to analyse the effects of condom use with application to Zimbabwe*, J. Math. Biol. **54** (2007), 669–699.
[29] Z. Mukandavire, S. Liao, J. Wang, H. Gaff, D. L. Smith, and J. G. Morris, *Estimating the reproductive numbers for the 2008–2009 cholera outbreaks in Zimbabwe*, Proceedings of the National Academy of Sciences of the United States of America **108** (2011), no. 21, 8767–8772.
[30] Y. Muroya, A. Bellen, Y. Enatsu, and Y. Nakata, *Global stability for a discrete epidemic model for disease with immunity and latency spreading in a heterogeneous host population*, Nonlinear Anal. Real World Appl. **13** (2012), no. 1, 258–274.
[31] A. Ramani, A. S. Carstea, R. Willox, and B. Grammaticos, *Oscillating epidemics: a discrete-time model*, Phys. A **333** (2004), no. 1, 278–292.
[32] J. Satsuma, R. Willox, A. Ramani, B. Grammaticos, and A. S. Carstea, *Extending the SIR epidemic model*, Phys. A **336** (2004), no. 3, 369–375.
[33] M. D. La Sen and S. Alonso-Quesada, *Some equilibrium, stability, instability and oscillatory results for an extended discrete epidemic model with evolution memory*, Adv. Difference Equ. **2013** (2013), 29 pp.
[34] M. Sekiguchi and E. Ishiwata, *Global dynamics of a discretized SIRS epidemic model with time delay*, J. Math. Anal. Appl. **371** (2010), no. 1, 195–202.
[35] A. Suryanto, W. M. Kusumawinahyu, I. Darti, and I. Yanti, *Dynamically consistent discrete epidemic model with modified saturated incidence rate*, Appl. Math. Comput. **32** (2013), no. 2, 373–383.
[36] J. H. Tien and D. J. D. Earn, *Multiple transmission pathways and disease dynamics in a waterborne pathogen model*, Bull. Math. Biol. **72** (2010), no. 6, 1502–1533.
[37] R. Villanueva, A. Arenas, and G. Gonzalez-Parra, *A nonstandard dynamically consistent numerical scheme applied to obesity dynamics*, J. Appl. Math. **2008** (2008), Art. ID 640154, 14 pp.
[38] J. Wang and S. Liao, *A generalized cholera model and epidemic-endemic analysis*, J. Biol. Dyn. **6** (2012), no. 2, 568–589.
[39] L. Wang, Z. Teng, and H. Jiang, *Global attractivity of a discrete SIRS epidemic model with standard incidence rate*, Math. Methods Appl. Sci. **36** (2013), no. 5, 601–619.
[40] World Health Organization. Available from: http://www.who.org.
[41] X. Zhou, J. Cui, and Z. Zhang, *Global results for a cholera model with imperfect vaccination*, J. Franklin Inst. **349** (2012), no. 3, 770–791.

Shu Liao
School of Mathematics and Statistics
Chongqing Technology and Business University
Chongqing, 400067, P. R. China
E-mail address: shuyang2011@yahoo.com

Weiming Yang
School of Mathematics and Statistics
Chongqing Technology and Business University
Chongqing, 400067, P. R. China
E-mail address: ywmctbu@gmail.com